Nonlinear Elastic J-Integral Measurements in Mode I Using a Tapered Double Cantilever Beam Geometry

David J. Macon*
ATK Launch Systems, PO Box 707, M/S 243, Brigham City, UT 84302-0707

Abstract

An expression for the J-integral of a nonlinear elastic material is derived for an advancing crack in a tapered double cantilever beam fracture specimen. The elastic and plastic fracture energies related to the test geometry and how these energies correlates to the crack position are discussed. The dimensionless shape factors η_{el} and η_p are shown to be equivalent and the deformation J-integral is analyzed in terms of the η_{el} function. The fracture results from a structural epoxy are interpreted using the discussed approach. The magnitude of the plastic dissipation is found to strongly depend upon the initial crack shape.

Key Words: J-integral, Plasticity, Cantilever beams, R-curve

*Corresponding Author. Tel.: (435)-863-3035, Email: david.macon@atk.com

Introduction

The fracture capability of adhesive joints has been greatly enhanced by the use of ductile adhesives. These materials show an increase in toughness with crack growth (a rising R-curve). Many of these materials including composites have been tested and modeled. One of the most commonly used test methods is the cantilever beam geometry [1]-[4]. The total J-integral of the bonded beams is measured, and the results are used in fracture models (e.g., cohesive zone models). In the works previously cited, the calculation of the J-integral is based on linear elastic beam theory [1]. The stiffness of the linear elastic beams is assumed to dominate any non-linear response from the adhesive. In this case, the J-integral is equal to the energy release rate.

ASTM D 3433 [5] covers the determination of the mode I energy release rate of adhesives using a double cantilever beam geometry. In addition, it includes instructions for using a tapered double cantilever beam (TDCB). The taper is designed so that the compliance of the beam is independent of crack length. Assuming that linear elastic beam theory applies, the only measured parameter required for establishing the energy release rate is the load. Also, the test method does not give any recommendation for introducing a sharp crack into the specimen. Specimen loading starts with a blunt crack. Once the crack starts propagating, the averaged load is used to calculate the energy release rate.

The test method described in ASTM D 3433 [5] does not explicitly calculate the toughening resulting from plastic deformation, which is a significant part of the

toughening mechanism. For rubber-toughened epoxies, the most significant part of the energy absorption results from cavitation of the particles and shear deformation of the epoxy matrix [6]-[9]. Subsequent unloading of the matrix also plays a significant part in the energy dissipative mechanism [10]. The characterization of these dissipative processes is an important part of understanding the fracture properties of an adhesive.

The intent of this paper is to measure the plastic component of the deformation J-integral for a growing crack for a double cantilever beam with a tapered geometry. The results are used to analyze the plastic J-integral of fracture data that was generated according to ASTM D 3433 [5]. The effect of precracking on the measured J-integral is also examined.

Deformation J-Integral

In an elastic material, the strain energy is independent of the loading history. The energy absorbed during crack growth in a nonlinear elastic material, however, exhibits history dependence. Rice developed a path independent approach called the J-integral to describe this behavior [11]. The J-integral defines the energy release rate for a nonlinear elastic material as

$$J = \frac{-\partial(U - F)}{\partial A} \tag{1}$$

where U is the strain energy stored in the body, F is the work done by external forces, and A is the crack area. The J-integral can be used for measuring fracture energy that is plastically dissipated during fracture in a material.

If the crack advances at a fixed displacement, there is no external work and Equation (1) reduces to

$$J = \frac{-\partial U}{\partial A} \tag{2}$$

The strain energy for a fixed displacement rate can be written as

$$U = \int_0^{\Delta} P d\Delta \tag{3}$$

where P is the applied load and Δ is the displacement.

Substituting Equation (3) into Equation (2) yields

$$J = -\int_0^{\Delta} \left(\frac{\partial P}{\partial A}\right)_{\Delta} d\Delta \tag{4}$$

If the specimen is of uniform width, B, with a crack of length, a, Equation (4) becomes

$$J = -\frac{1}{B}\int_0^{\Delta}\left(\frac{\partial P}{\partial a}\right)_{\Delta} d\Delta \tag{5}$$

Ernst et al. [12] proposed that the load can be written as separable multiplicative functions as

$$P = F(\Delta)H(a) \tag{6}$$

where $F(\Delta)$ is a function of displacement and $H(a)$ is a function of crack length.

If the deformation is restricted to the remaining ligament length, b, Equation (6) can be rewritten as

$$P = F(\Delta)K(b) \tag{7}$$

where $K(b)$ is a function of ligament length. By noting that $\partial a = -\partial b$, one can obtain $\frac{\partial P}{\partial a}$ from differentiation of Equation (7)

$$\frac{\partial P}{\partial a} = -\frac{\partial P}{\partial b} = -\left[K(b)\frac{\partial F(\Delta)}{\partial b} + F(\Delta)\frac{\partial K(b)}{\partial b}\right] = -F(\Delta)\frac{\partial K(b)}{\partial b} = -\frac{P}{K(b)}\frac{\partial K(b)}{\partial b} \tag{8}$$

Substitution into Equation (5) gives

$$J = \frac{1}{BK(b)} \frac{\partial K(b)}{\partial b} \int_0^{\Delta} P d\Delta \tag{9}$$

Equation (9) is often written as [13]

$$J = \frac{\eta}{Bb} \int_0^{\Delta} P d\Delta \tag{10}$$

where $\eta = \frac{b}{K(b)} \frac{\partial K(b)}{\partial b}$. The J-integral is often divided into an elastic and plastic component [14]

$$J = \frac{\eta_{el}}{Bb} \int_0^{\Delta_{el}} P d\Delta_{el} + \frac{\eta_p}{Bb} \int_{\Delta_{el}}^{\Delta_p} P d\Delta_p \tag{11}$$

where the el and p subscripts refer to the elastic and plastic contributions, respectively. The use of Equation (11) allows the elastic and plastic contribution of the total J-integral to be established, assuming that the dimensionless constants η_{el} and η_p are known.

So far the discussion has been restricted to a static crack. When the crack starts to advance, a significant portion of the stored energy is released in the plastic wake that forms behind the growing crack [10]. Consequently, an unambiguous definition of

energy release rate does not exist for a crack growing in a nonlinear elastic material. One common approach is to define a psuedo energy release rate called the deformation J-integral [15], which equals the rate of energy dissipated as the crack advances. This can be illustrated by considering a crack that has grown to a length a_2 from an initial length a_1. This is illustrated in Figure 1. The top line shows the actual loading path. As the crack advances from a_1 to a_2, energy is stored by the material and also dissipated in a plastic wake that forms behind the growing crack. The "actual loading path" no longer contains the accurate path for calculating the J-integral. The accurate description is given by a "deformation path", which is equivalent to loading the specimen again from scratch but at crack length a_2. The area under curve OAB represents the strain energy in an elastic material with crack length a_1. The area under curve OCD then represents the elastic strain energy for crack length a_2. This strain energy is denoted, U_D, where the subscript D refers to deformation theory. In Figure 1, U_D is the area under the "deformation path" for the appropriate crack length.

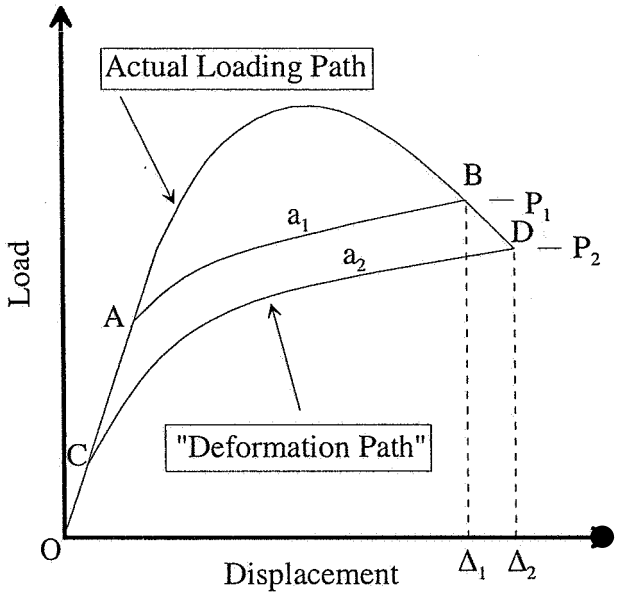

Figure 1. Load versus displacement curve for deformation J-integrals.

A deformation J-integral, J_D for a nonlinear elastic body with a growing crack can be defined as

$$J_D = -\frac{1}{B}\left(\frac{\partial U_D}{\partial a}\right)_{\Delta} \tag{12}$$

Equation (12) can be rewritten in the following form

$$J_D = \frac{\eta U_D}{Bb} \tag{13}$$

The terms η, b, and U_D will change as the crack length grows. The deformation J-integral can also be divided into an elastic and plastic contribution. The plastic

component of deformation J-integral, J_{Dp}, is calculated incrementally from the following relation [15]

$$J_{Dp_i} = \left[J_{Dp_{i-1}} + \left(\frac{\eta_{pi-1}}{Bb_{i-1}} \right) \frac{(P_i + P_{i-1})(\Delta_{pi} - \Delta_{pi-1})}{2} \right] \left(1 - \gamma_{i-1} \frac{a_i - a_{i-1}}{b_{i-1}} \right) \tag{14}$$

where P is the load, Δ_p is the plastic displacement, and $\gamma = \left(\eta_p - 1 + \frac{b}{\eta_p} \frac{\partial \eta_p}{\partial b} \right)$. The relation given above is an approximation and simplifying assumptions were used in its derivation. ASTM E 1820 [16] uses this approach for the calculation of J-R curves. The η_p term needs to be evaluated as a function of crack length (or equivalently for ligament length) for the TDCB geometry. The notation denoting the deformation J-integral will be dropped with the implied assumption that the J-integral for an advancing crack is the deformation J-integral.

η Derivation for a TDCB Geometry

The η term described by Equation (10) allows calculation of the J-integral based on experimental load and displacement data. The η parameter is dependent on the fracture test geometry. The J-integral can be separated into elastic and plastic components as,

$$J = J_{el} + J_p = \frac{\eta_{el} U_{el}}{Bb} + \frac{\eta_p U_p}{Bb} \tag{15}$$

The η_{el} and η_p parameters are not necessarily equal to each other, and must be determined independently or shown to be equivalent.

For the double cantilever beam, η_{el} can be found by considering the compliance, C, of the beams. Mostovoy et al. [17] calculated the compliance of beams by considering the contributions from bending and shear deflections as

$$C = \frac{\Delta}{P} = \frac{8}{EB}\left[\frac{a^3}{h^3} + \frac{a}{h}\right] \tag{16}$$

where E is Young's modulus, and h is the beam height at a distance, a, from the point of loading. They proposed that if the beam geometry were designed so that the compliance changed linearly with crack growth, dC/da would be constant. The term in brackets is set equal to a geometric factor, m, and for this set of tests is equal to 35.43 cm^{-1} [5]. Equation (16) assumes that the ends of the beam were "built-in" and that no rotation resulted. To correct this, they changed the crack length to $a_F = a + a_o$, where a_o is an empirical rotation correction. Kanninen [18] evaluated a_o by considering the cantilever beam as being supported on a compliant foundation and found

$$a_o \approx 0.64h \tag{17}$$

Blackman et al. [19] used this result along with additional derivations to derive a compliance expression for the TDCB adherend as

$$C = \frac{8m}{EB}\left[a + 0.64\left(\frac{3}{m}\right)^{1/3} a^{2/3} - \frac{2}{3}x_o\right] \tag{18}$$

where x_o is a constant that represents the length of the straight section of the beam running from the load point to the beginning of the taper. The expression given in Equation (18) corrects for the effects of beam root rotation and for the actual profile of the TDCB adherend.

For linear elastic conditions, the elastic component of the J-integral, J_{el}, is the same as the energy release rate, G, and can be found using the compliance expression given in Equation (18)

$$J_{el} = G = \frac{P^2}{2B}\frac{\partial C}{\partial a} = \frac{P\Delta_{el}}{2}\frac{1}{BC}\frac{\partial C}{\partial a} \tag{19}$$

where $U_{el} = \frac{P\Delta_{el}}{2}$ and $\eta_{el} = \frac{b}{C}\left(\frac{\partial C}{\partial a}\right)$.

To find η_p, a separable form for the load function is chosen as $P = F(\Delta_p)G(a_F)$. The function, $G(a_F)$, is set equal to the reciprocal compliance given in Equation (18)

$$G(a_F) = C^{-1} = \frac{EB}{8m}\left[a + 0.64\left(\frac{3}{m}\right)^{1/3} a^{2/3} - \frac{2}{3}x_o\right]^{-1} \tag{20}$$

This leaves an undefined function of displacement, $F(\Delta_p)$. Substituting this definition of load into Equation (5) gives

$$J_p = -\frac{1}{B}\int_{\Delta_{el}}^{\Delta_p}\left[\frac{\partial}{\partial a}\left(C^{-1}F(\Delta_p)\right)d\Delta\right]$$

$$= \frac{1}{BC^2}\frac{\partial C}{\partial a}\int_{\Delta_{el}}^{\Delta_p} F(\Delta_p)\,d\Delta$$

The integration limits are only chosen over displacements where plastic dissipation occurs.

By noting that $P = F(\Delta_p)G(a_F)$ and using Equation (20), the plastic contribution to the J-integral becomes

$$J_p = \frac{1}{BC}\frac{\partial C}{\partial a}\int_{\Delta_{el}}^{\Delta_p} P\,d\Delta \tag{21}$$

Then, $J_p = \frac{\eta_p U_p}{Bb}$ where $U_p = \int_{\Delta_{el}}^{\Delta_p} P d\Delta$ and $\eta_p = \frac{b}{C}\left(\frac{\partial C}{\partial a}\right)$. For the tapered double cantilever beam geometry, $\eta_p = \eta_{el}$ assuming that the compliance is not a function of displacement. The compliance function given in Equation (20) assumes linear elastic response of the beams, which is accurate for the experimental data presented in this paper. This derivation followed the approach given by Krasovskii et al. [20] where the same conclusion was reached for the straight double cantilever beam geometry.

Experimental

The J-integral approach was tested using cantilever beams of the tapered variety. The beams were made of D6AC steel and conformed to ASTM D 3433 [5]. A schematic of the specimen is shown in Figure 2.

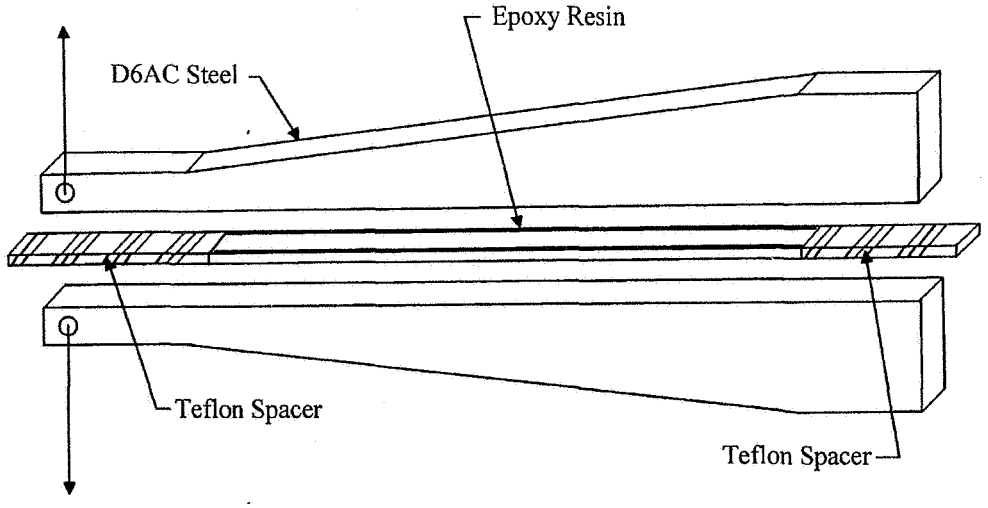

Figure 2. Geometry of the tapered double cantilever beam specimens.

The tapered double cantilever beam (TDCB) adherends were bonded using a thixotropic structural epoxy, TIGA 321®, manufactured by Resin Technology Group (RTG). The structure properties of this adhesive have been discussed elsewhere [21]-[23]. Excess adhesive was applied to each beam and allowed to extrude out as the two adherends were pressed together. The extruded adhesive was removed from the side of the beams prior to curing. The bondline thickness was maintained at 0.127 cm using Teflon® spacers controlled to a 10% dimensional tolerance. After bonding, the specimens were placed in a jig that helped maintain alignment and a slight compressive load was applied. After an elevated temperature cure, the specimens were allowed to equilibrate at 22°C.

Crack propagation gages [24] were applied to the adherends using TIGA 321®. In the tear region of the gage, adhesive was allowed to fully encapsulate the exposed conductive elements. This helped ensure that the crack propagation gage failed at the same rate as the TDCB specimen. After bonding the gages, the adhesive was cured at the same elevated temperature. The displacement was evaluated using clip on gages. Each gage was calibrated prior to testing.

The bonded adherends were tested using a Satec® Unidrive. The tests were performed at cross-head speeds of 0.0127 cm/min. Test temperatures of 22°C and 46°C were selected. An environmental chamber was used in conjunction with the Unidrive when temperature testing was required.

Calculation of η_{el}

The η_{el} (and hence η_p) shape factor used to calculate J_{el} was derived using finite element (FE) analysis. The η_{el} term was derived using ABAQUS FE code with a two-dimensional model of the tapered double cantilever beam with linear-elastic material constants. Eight-node plain-strain quadratic elements were used. Elastic constants of $E = 204$ GPa and $\upsilon = 0.33$ were used for the steel. The adhesive used $E = 3.31$ GPa and $\upsilon = 0.38$ for TIGA 321® at 22°C, and $E = 1.72$ GPa and $\upsilon = 0.41$ for TIGA 321® at 46°C. An applied load of 4960 N and an adhesive thickness of 0.127 cm was used in the FEA modeling. The ligament length prior to crack growth is 17.9 cm. The η_{el} is calculated from J_{el} using the following expression

$$\eta_{el} = \frac{J_{el} B b}{U_{el}} \tag{22}$$

For a linear elastic material, U_{el} can be written as $U_{el} = \frac{P\Delta_{el}}{2}$. The elastic displacement, Δ_{el}, can be calculated with FEA.

Figure 3 shows the FEA calculated elastic J-integral versus a for bondlines of TIGA 321® at 22°C and 46°C. The figure includes the calculated J-integral for a steel bondline. Inspection of the figure shows that the shape of the J_{el} curves increases slightly as short crack length and then decreases until the crack length approaches 10 cm. At this crack length value, there is a sharp increase in J-integral value.

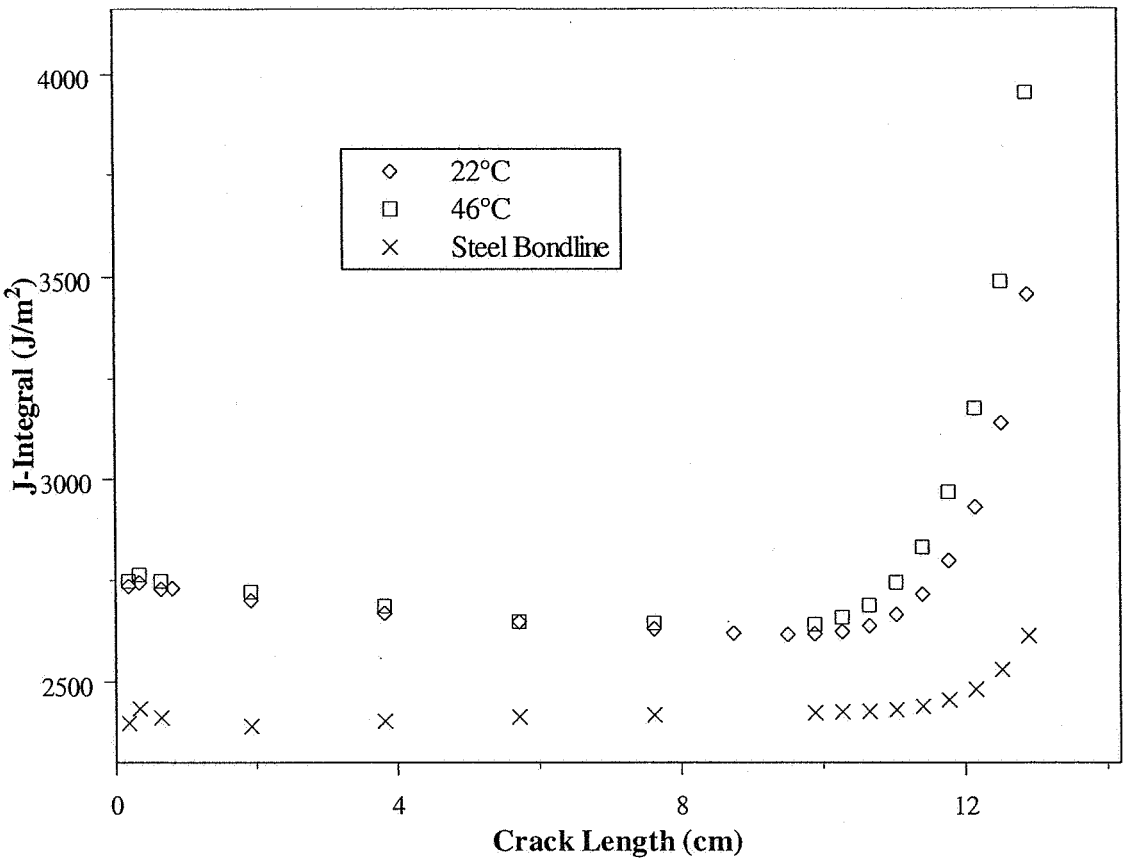

Figure 3. Linear-elastic J-integral versus crack length as calculated from FEA.

Unlike G_c, the calculated J-integral for the TDCB adherend is not independent of crack length. FEA calculations predict that the adhesive bondline is subjected to a fairly uniform strain energy level until the crack length approaches 10 cm. At that length, the input strain energy value increases rapidly to a magnitude that depends upon the bondline material. Experimental results support these conclusions. TIGA 321® tested at 22°C and at a crosshead displacement of 0.0127 cm/minute has stable crack propagation until crack lengths ranging from 8.9-11.4 cm are reached. At which point, the crack propagation suddenly becomes unstable. This is associated with the adhesive no longer being able to stably dissipate the increase in strain energy.

The dimensionless η_{el} parameter is calculated using Equation (22). The η_{el} function versus crack length is shown in Figure 4. From the figure, it can be seen that there is a slight dependence upon the bondline properties at short crack lengths. This dependence decreases with increasing crack length until a crack length of 10 cm is approached at which point the η_{el} values begin to diverge again. All J-integral calculations involving η_{el} will be based upon TIGA 321® at 72°F.

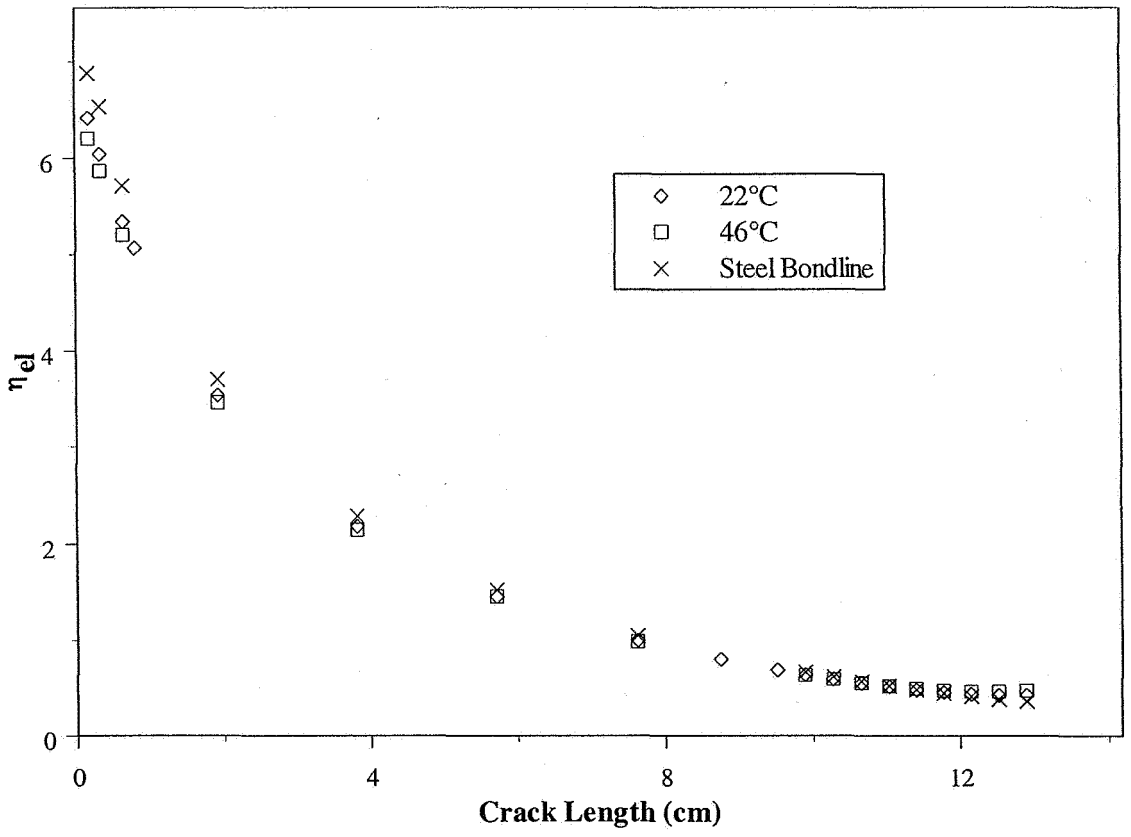

Figure 4. η_{el} versus a for the TDCB geometry

Table 1 contains J_{el}, Δ_{el}, and η_{el} for TIGA 321® at 22°C. Interpolations between data points are easily done by a variety of mathematical methods.

Table 1. J_{el}, Δ_{el}, and η_{el} for the TDCB geometry with TIGA 321® at 22°F.

a (cm)	η_{el}	J_{el} (J/m^2)	Δ_{el} (cm)
0.183	6.391	2735.48	0.0777
0.338	6.022	2744.24	0.0820
0.648	5.318	2728.48	0.0907
0.808	5.049	2730.23	0.0947
1.923	3.523	2700.46	0.1255
3.820	2.172	2668.93	0.1773
5.712	1.447	2647.92	0.2286
7.617	0.992	2630.40	0.2794
8.745	0.793	2619.90	0.3099
9.505	0.682	2616.39	0.3302
9.886	0.632	2618.15	0.3404
10.267	0.586	2623.40	0.3505
10.648	0.544	2637.41	0.3607
11.029	0.506	2665.43	0.3708
11.402	0.475	2716.22	0.3810
11.775	0.449	2798.53	0.3912
12.146	0.431	2931.62	0.4013
12.520	0.419	3140.02	0.4140
12.891	0.419	3457.00	0.4242

Accuracy of the finite element model

A comparison was conducted between the compliance expression given in Equation (18) and the ABAQUS FE model. Eight-node biquadratic plane stress elements were assigned to the metallic beams. Similar nodes were assigned to the adhesive bondline except that plane strain elements were chosen. The beam elements were assigned linear elastic behavior. The adhesive elements were assumed to follow a Ramberg-Osgood plasticity model (deformation plasticity behavior in the ABAQUS model). The compliance of the FE model beam was determined.

Figure 5 shows the calculated compliance from the Blackman model (Equation (18)) along with the compliance from FE calculations. The agreement between the two curves is excellent. The implication is that FE model behaves as expected.

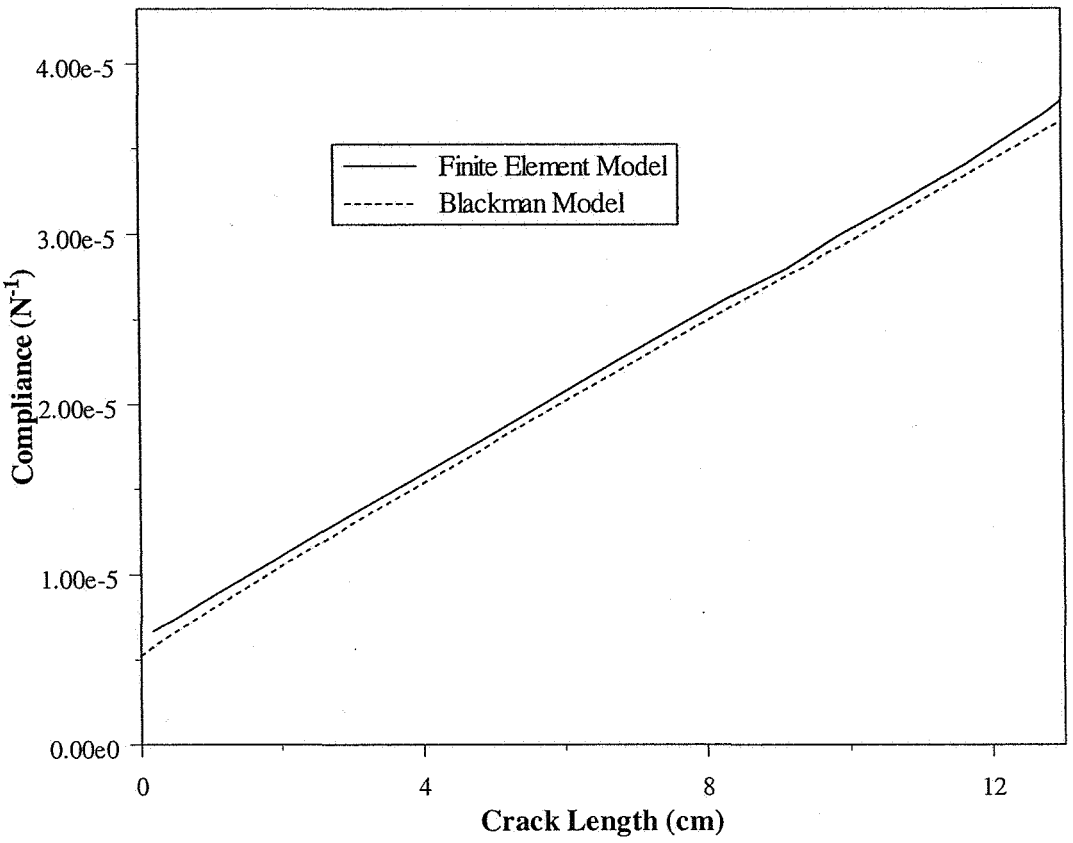

Figure 5. Compliance versus crack length for Blackman and FE models.

Results

22°C Fracture Testing Results

The load versus time trace for a TDCB adherend tested at 0.127 cm/min and 22°C is shown in Figure 6. Included in the illustration is the crack location as a function of time. It can be seen that the crack velocity is fairly constant until a crack length of 8.76 cm is reached. At which point, the crack growth suddenly becomes unstable.

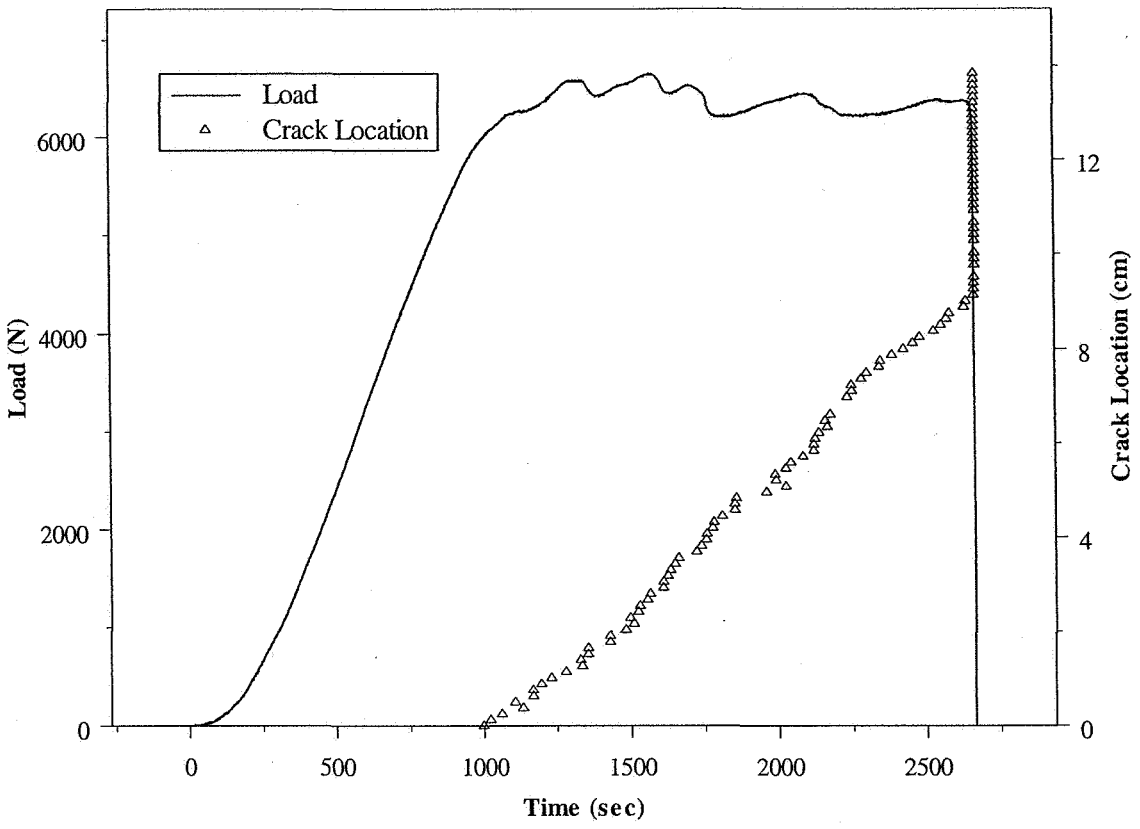

Figure 6. Plot of load and crack position versus time for a TDCB specimen tested at 22°C.

Typical geometries used for generating R-curves are of the single edge notch bend (SENB) or deeply notched compact specimen varieties. These specimens are designed for testing bulk material and are assumed to have sharp cracks. In the case of the TDCB geometry, the specimen is more representative of the adhesive bondline. Ever since Bascom et al. [25] showed a strong dependence of critical strain energy on adhesive thickness, cantilever beam geometries have been a logical choice for characterizing the fracture behavior of adhesives.

The J-integral up to the point of crack growth (~1000 seconds) can be calculated using Equation (11). The elastic displacement is calculated using FEA for each experimental

load value. The plastic displacement is found by subtracting the calculated elastic displacement from the total experimental displacement. Once the crack starts advancing, the plastic component of the J-integral is calculated using Equation (14). The total J-integral represents the summation of the elastic and plastic components. In calculating the J-integral, a smoothing algorithm was applied to the load and displacement data. Specifically, a routine was applied to both data sets through the piecewise use of a symmetric *k*-nearest neighbor linear square fitting in which *k* is adaptively chosen.

Figure 7 shows the calculated R-curve, which depicts the total J-integral, elastic J-integral, and plastic J-integral versus crack length. Inspection of the figure shows a decrease in the total J-integral with increasing crack length. The plastic component of the J-integral also declines with increasing crack growth. The elastic component increases with increasing crack growth in a profile typical for R-curves. However the total J-integral is atypical. A normal R-curve profile increases in magnitude. In this case, the magnitude of the plastic component at small crack lengths represents a significant portion (~44%) of the total J-integral. At crack lengths approaching 2.54 cm, the elastic component begins to dominate.

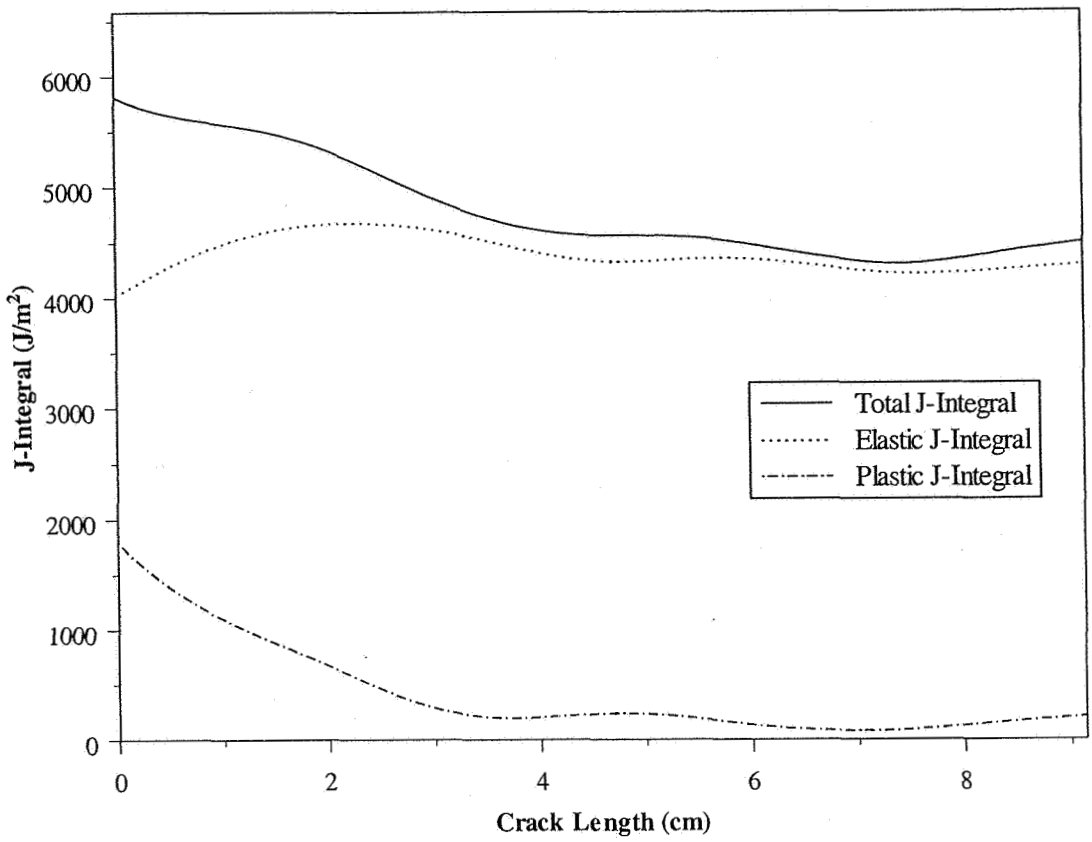

Figure 7. J-integral for TIGA 321® tested at 22°C.

The TDCB geometry described in ASTM D 3433-99 [5] assumes that "this test method depends upon the establishment of a sharp-crack condition in the bondline in a specimen of adequate size." No recommendations are given on how to precrack TDCB adherends. For data reported in this section, no precracking took place. The initial crack resulted from a blunt face starting at the leading edge of the adhesive bondline. This was modeled for the TDCB geometry using FEA analysis. The adhesive was assumed to follow the Ramberg-Osgood plasticity model. The results are shown in Figure 8, which depicts the plastic strain for mode I opening. The greatest amount of plastic strain occurs just prior to crack initiation. Once the crack starts to propagate, the extent of plastic strain decreases. This trend continues until a "steady-state" is reached. This would support the

observation shown in Figure 7 where the greatest amount of plastic dissipation occurs just prior to crack growth.

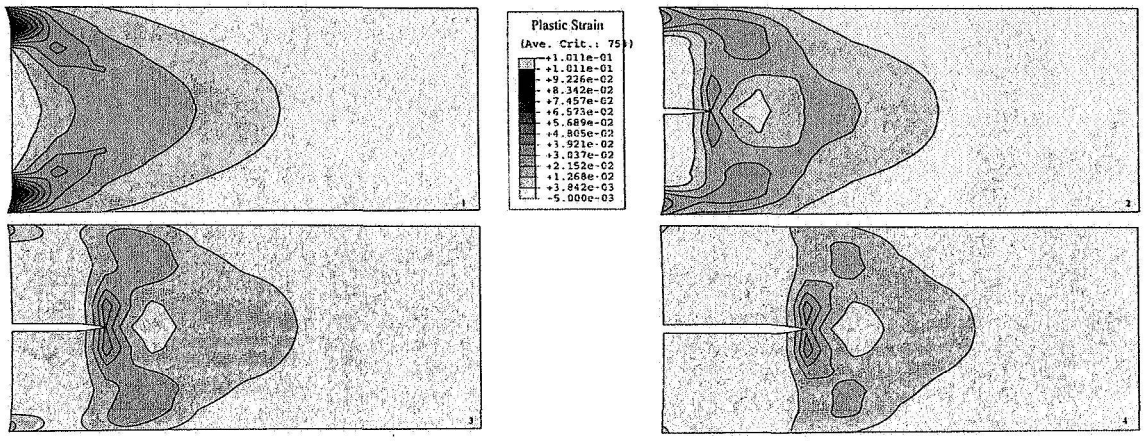

Figure 8. Plastic strain profile for mode I opening an advancing crack in TIGA 321® using a Ramberg-Osgood plasticity model

46°C Fracture Testing Results

The load and crack position versus time profile for an adherend tested at 46°C and 0.0127 cm/min is shown in Figure 9. At this test temperature, the material strengthens significantly from a crack initiation load of approximately 4900 N up to a stable crack propagation load of approximately 11000 N. This represents an increase in load of over 225%. Catastrophic failure occurs at a crack length approaching 9.5 cm as predicted by FEA analysis. The load increase from 4900 N to 11000 N represents a critical strain energy increase of over 500%.

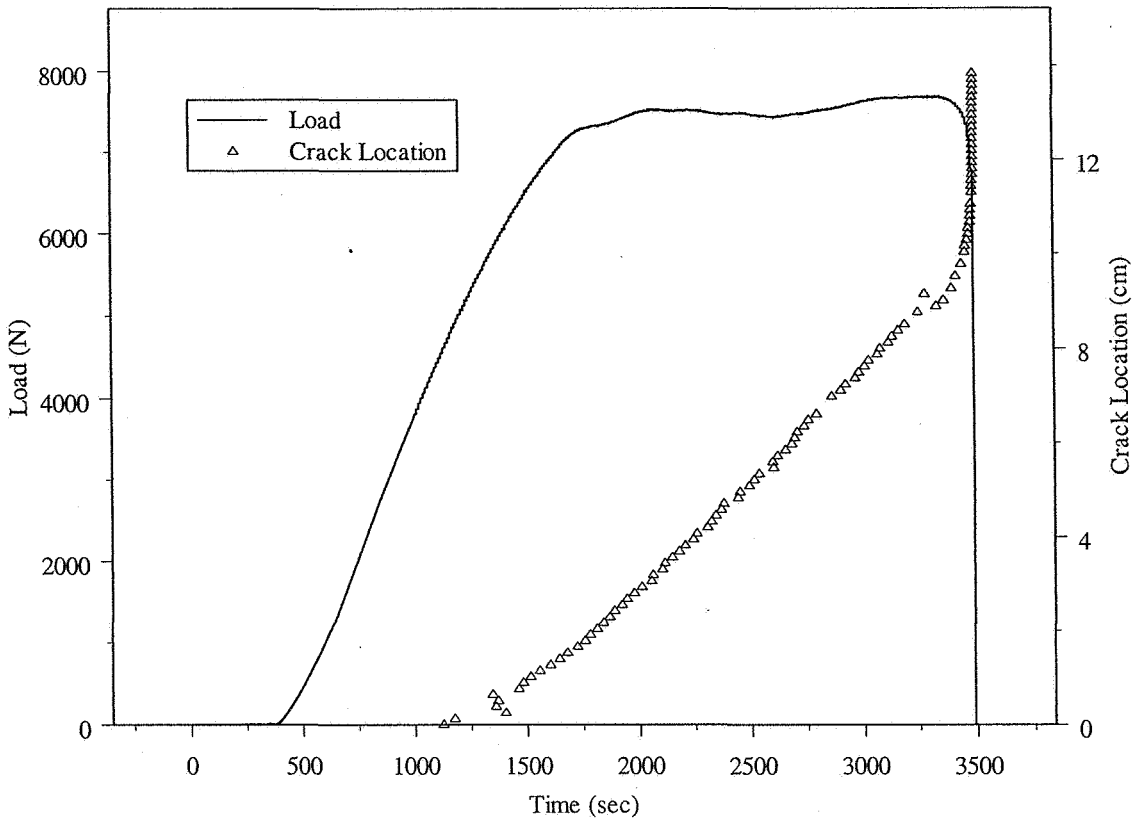

Figure 9. Load and crack position profile for TIGA 321® tested at 46°C

The calculated J-integral values are depicted in Figure 10. The total J-integral, elastic J-integral, and plastic J-integral are shown versus crack length. This J-integral profile is significantly different when compared to the curves generated at 22°C. The total and elastic J-integrals show an increasing R-curve type profile. The plastic J-integral decreases again with increasing crack growth but the overall magnitude is much less. This result might be expected because the glass transition temperature of TIGA 321® is being approached (~51.7°C). As the adhesive becomes softer and rubbery, the material undergoes less irreversible deformation. The plastic J-integral also reaches some negative values and is representative of the errors associated with Equation (14).

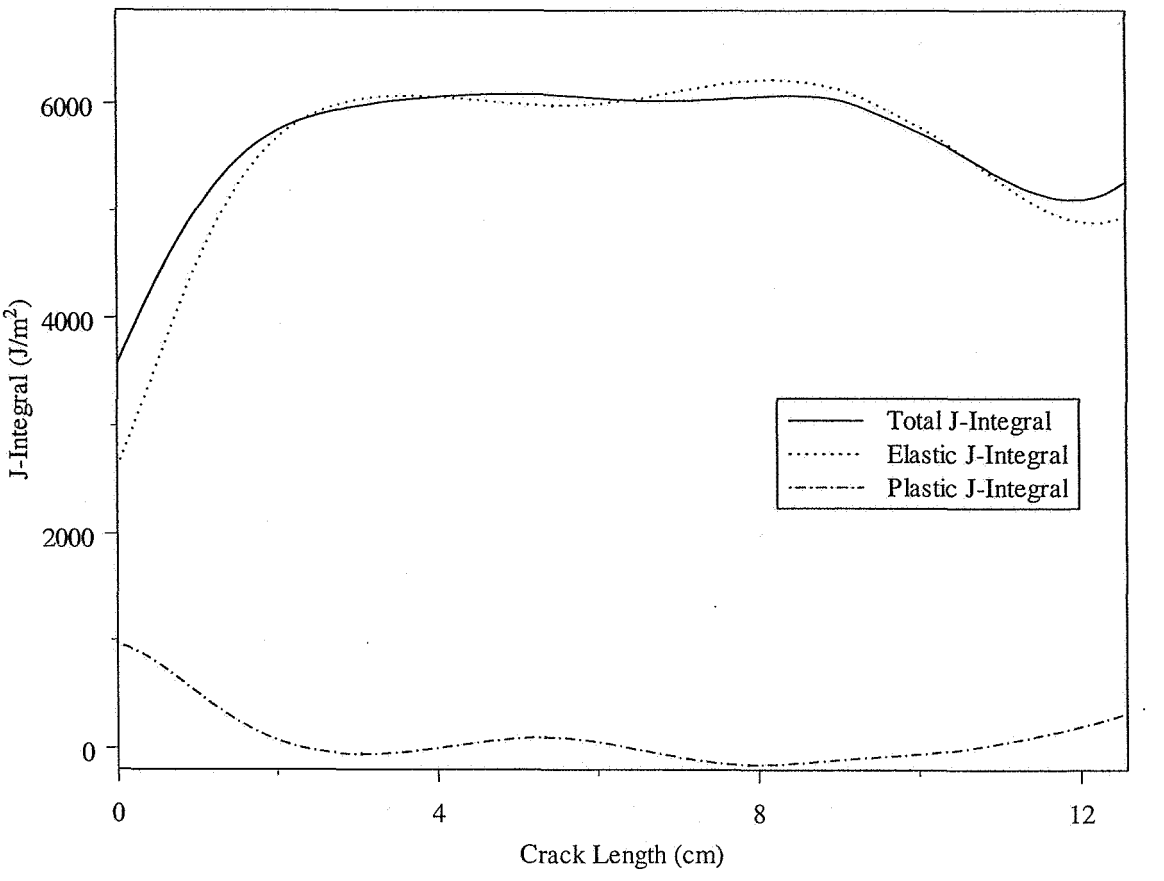

Figure 10. J-integral for TIGA 321® tested at 46°F.

Precracking of TDCB Specimens

The effect of precracking on TDCB adherends was examined. A group of seven TDCB specimens was precracked by loading the adherends to 80% of their critical fracture load. Liquid nitrogen was then sprayed on the leading edge of the adhesive. This resulted in a sharp crack that jumped approximately 2 cm through the center of the adhesive. Another group of seven TDCB specimens was precracked by placing a PTFE film (~0.008 cm thickness) in the center of the adhesive bondline at the leading edge. Both precracked sets were pulled at 0.127 cm/min and 22°C.

Table 2 contains a summary of the plastic contribution to the total J-integral prior to crack initiation for these specimen sets. Included in the table are the results from a group of seven test specimens that were not precracked. Inspection of the table shows that the PTFE insert group was statistically equivalent to the specimens that were not precracked. The group precracked with liquid nitrogen showed a significant drop in plastic dissipation prior to crack growth when compared to the other groups. The latter method appears to be the more effective method for introducing a sharp crack. It should be noted that the bondlines used in this study were significantly thicker than bondlines tested elsewhere (e.g., 0.127 cm reported here versus 0.015 cm reported by Blackman et al. [19]). The thicker bondlines will allow more plastic deformation of the process zone and make the specimen more sensitive to precracking methods.

Table 2. Averaged plastic J-integral contribution to the total J-integral just prior to crack growth. The standard deviation from a total of seven specimens per test group is included in the table.

Precracking method	No precrack	PTFE insert	Liquid N_2 precrack
Percent Plastic contribution	$42.6 \pm 3.0\%$	$39.7 \pm 4.4\%$	$7.27 \pm 1.7\%$

Conclusion

A method for measuring the total J-integral for a TDCB adherend was described. Also included was an approach for evaluating the elastic and plastic contribution to the J-integral. An η_{el} function for the TDCB geometry was evaluated using FEA, and was shown to be equivalent to η_p. Testing showed that TDCB adherends with a blunt edge

had significant plastic deformation prior to crack growth. The plastic deformation decreased as the crack advanced. In addition, the extent of plastic deformation decreased as the glass transition temperature was approached.

The ASTM describing TDCB testing recommends precracking but gives no suggestions on how to accomplish this. PTFE inserts did little to alter J_p prior to crack growth. Loading the specimen and spraying the leading edge with liquid nitrogen sharply reduced the plastic deformation prior to crack growth. For the limited number of approaches reported here, precracking with liquid nitrogen gave the sharpest cracks.

[1] Suo Z, Bao G, Fan B. Delamination R-curve phenomena due to damage. J Mech Phys Solids. 1992;40(1):1-16.

[2] Sorensen BF, Jacobsen TK. Determination of cohesive laws by the J integral approach. Eng Fract Mech. 2003;70:1841-1858.

[3] Sorensen BF. Cohesive law and notch sensitivity of adhesive joints. Acta Mat. 2002;50:1053-1061.

[4] Jacobsen TK, Sorensen BF. Mode I intra-laminar crack growth in composites - modeling of R-curves from measured bridging laws. Composites Part A. 2001;32:1-11.

[5] ASTM, ASTM D 3433-99. Standard test method for fracture strength in cleavage of adhesives in bonded metal joints. American Society for Testing and Materials, Philadelphia, PA, 1999.

[6] Kinloch AJ, Shaw SJ, Tod DA, Hunston DL. Deformation and fracture behavior of a rubber-modified epoxy: 1. Microstructure and fracture studies. Polymer. 1983;24:1341-1354.

[7] Kinloch AJ, Shaw SJ, Tod DA, Hunston DL. Deformation and fracture behavior of a rubber-modified epoxy: 1. Microstructure and fracture studies. Polymer. 1983;24:1355-1363.

[8] Evans AG, Ahmad ZB, Gilbert DG, Beaumont PWR. Mechanisms of toughening in rubber-toughened polymers. Acta Mater. 1986;34:79-87.

[9] Yee AF, Li D, Li X. The importance of constraint releif causes by rubber cavitation in the toughening of epoxy. J Mat Sci. 1993;28:6392-6398.

[10] Du J, Thouless MD, Yee AF. Development of a process zone in rubber-modified epoxy polymers. Int J Frac. 1998;92:271-285.

[11] Rice JR. A path independent integral and the approximate analysis of strain concentration by notches and cracks. J App Mech. 1968;35:379-386.

[12] Ernst HA, Paris PC, Rossow M, Hutchinson JW. Analysis of load-displacement relationships to determine J-R curve and tearing instability material properties. In Fracture Mechanics. ASTM STP 677, 1979. p. 581-599.

[13] Sharobeam MH, Landes JD. The load separation and η_{pl} development in precracked specimen test records. Int J Fract. 1993;59:213-226.

[14] Sumpter JPG, Turner CE. Method for laboratory determination of Jc (contour integral for fracture analysis). In Cracks and Fracture, ASTM STP 601, 1976. p. 3-15.

[15] Anderson TL. Fracture Mechanics: Fundaments and Applications. Boca Raton: CRC Press, 1995.

[16] ASTM, ASTM E 1820-01. Standard test method for measurement of fracture toughness. American Society for Testing and Materials, Philadelphia, PA, 2001.

[17] Mostovoy S, Crosley PB, Ripling EJ. Use of crack-line-loaded specimens for measuring plain-strain fracture toughness. J Mats. 1967;2(3):661-681.

[18] Kanninen MF. An augmented double cantilever beam model for studying crack propagation and arrest. Int J Fract. 1973;9(1):83-92.

[19] Blackman BRK, Hadavinia H, Kinloch AJ, Paraschi M, Williams JG. The calculation of adhesive fracture energies in mode I: revisiting the tapered double cantilever beam (TDCB) test. Eng Fract Mech 2003;70:233-248.

[20] Krasovskii AY, Torop VM, Orynyak IV, Kalaida VV. Determination of the J-integral on double cantilever beam specimens at crack start and arrest," Soviet Mats Sci. 1986;22(2):144-150.

[21] Richardson DE, Anderson GL, Macon, DJ. Multi-axial loading failure criterion for isotropic, time-dependent materials. Int J Adhes Adhes. 2004;24(3):211-217.

[22] Macon DJ, Anderson AG. Kinetic energy corrections for slip-stick behavior in brittle adhesives. J App Poly Sci. 2002;86(8):1821-1828.

[23] Macon DJ. Effective adhesive modulus approach for evaluation of curing stresses.. Polymer. 2001;42(12):5285-5291.

[24] Macon DJ, Totman PD, Bodily ML, Everton RL, Eggett MR. Development of a low data event timer for monitoring an advancing crack in fracture. Int J Adhes Adhes. 2005;25(6):475-483.

[25] Bascom WD, Cottington RL, Jones RL, Peyser P. The fracture of epoxy- and elastomer- modified epoxies in bulk and as adhesives. J App. Poly. Sci. 1975;19:2545-2462.

Table 3. J_{el}, Δ_{el}, and η_{el} for the TDCB geometry with TIGA 321® at 22°F.

a (cm)	η_{el}	J_{el} (J/m^2)	Δ_{el} (cm)
0.183	6.391	2735.48	0.0777
0.338	6.022	2744.24	0.0820
0.648	5.318	2728.48	0.0907
0.808	5.049	2730.23	0.0947
1.923	3.523	2700.46	0.1255
3.820	2.172	2668.93	0.1773
5.712	1.447	2647.92	0.2286
7.617	0.992	2630.40	0.2794
8.745	0.793	2619.90	0.3099
9.505	0.682	2616.39	0.3302
9.886	0.632	2618.15	0.3404
10.267	0.586	2623.40	0.3505
10.648	0.544	2637.41	0.3607
11.029	0.506	2665.43	0.3708
11.402	0.475	2716.22	0.3810
11.775	0.449	2798.53	0.3912
12.146	0.431	2931.62	0.4013
12.520	0.419	3140.02	0.4140
12.891	0.419	3457.00	0.4242

Table 4. Averaged plastic J-integral contribution to the total J-integral. Standard deviation is included.

Precracking method	Blunt crack	PTFE insert	Liquid N_2
J_p percent contribution	42.6 ± 3.0	39.7 ± 4.4	7.27 ± 1.7